Conversion of native grasslands into croplands in the Pampa biome and its effects on source contributions to suspended sediment of the Ibirapuitã River, Brazil

Rafael Ramon, Olivier Evrard, Sylvain Huon, Carlos Eduardo Linhares Feitosa, Felipe Bernardi, Antônio Augusto Medeiros Batista, Tadeu Luis Tiecher, Jean Paolo Gomes Minella, Cláudia Alessandra Peixoto Barros, Tales Tiecher

Conversion of native grasslands into croplands in the Pampa biome and its effects on source contributions to suspended sediment of the Ibirapuitã River, Brazil

Rafael Ramon[1,2,*] | Olivier Evrard[2] | Sylvain Huon[3] | Carlos Eduardo Linhares Feitosa[1] | Felipe Bernardi[4] | Antônio Augusto Medeiros Batista[5] | Tadeu Luis Tiecher[6] | Jean Paolo Gomes Minella[7] | Cláudia Alessandra Peixoto Barros[8] | Tales Tiecher[8]

Correspondence
Department of Soil Science, Universidade Federal do Rio Grande do Sul, Porto Alegre, RS, Brazil. E-mail: tales.tiecher@ufrgs.br

[1] *Graduate Program in Soil Science, Universidade Federal do Rio Grande do Sul, Bento Gonçalves Ave., 91540-000 Porto Alegre, RS, Brazil – Interdisciplinary Research Group on Environmental Biogeochemistry - IRGEB (rafaramon11@gmail.com, eduardo.linhares@live.com), [*]Current affiliation: BASF SA, Environmental Fate - Regulatory Science Crop Protection, Avenida Brasil, 791, Guaratinguetá - São Paulo, Brazil.*

[2] *Laboratoire des Sciences et de l'Environnement, UMR 8212 (CEA/CNRS/UVSQ-IPSL), 91 191 Gif-sur-Yvette Cedex (France), Université Paris-Saclay, France – IRGEB (olivier.evrard@lsce.ipsl.fr)*

[3] *Sorbonne Universités UPMC Univ Paris 06, Institut d'Ecologie et des Sciences de l'environnement de Paris (iEES), 4 place Jussieu, 75 252 Paris cedex 05, France (sylvain.huon@sorbonne-universite.fr)*

[4] *Graduate Program in Soil Science, Universidade Federal de Santa Maria, Roraima Ave. 1000, 97105-900 Santa Maria, RS, Brazil (felipekbernardi@gmail.com)*

[5] *Farroupilha Federal Institute of Education, Science and Technology (IFFar), 97555-000 Alegrete, RS, Brazil (augustomarquez112@gmail.com)*

[6] *Rio Grande do Sul Federal Institute, Campus Restinga, 91791-508, Porto Alegre, RS, Brazil (tadeu.t@hotmail.com)*

[7] *Department of Soil Science, Universidade Federal de Santa Maria, Roraima Ave. 1000, 97105-900 Santa Maria, RS, Brazil (jminella@gmail.com)*

[8] *Department of Soil Science, Universidade Federal do Rio Grande do Sul, Bento Gonçalves Ave. 7712, 91540-000 Porto Alegre, RS, Brazil (claudia.barros@ufrgs.br; tales.tiecher@gmail.com)*

Short running title

Pampa grassland-to-cropland conversion impact on Ibirapuitã River

Abstract

Grain crops have expanded at the expense of native grasslands in South America's Pampa Biome in recent decades, thereby increasing the sediment delivery to the river systems. This study aimed to evaluate the impact of land use change on sediment sources contributions in the Ibirapuitã catchment (5,942 km²), Southern Brazil. For this purpose, a sediment fingerprinting approach was developed based on organic matter composition, ultra-violet-visible reflectance, and fallout radionuclide activities as potential tracers. Four main sediment sources were investigated: croplands (*n*=36), native grasslands (*n*=31), unpaved roads (*n*=31), and subsurface sources (*n*=34). Tracers were selected following a three-step procedure: conservative range test, Kruskal–Wallis H-test, and linear discriminant function analysis (LDA). Selected tracers were introduced into a mass balance mixing model to estimate the source contributions to in-stream sediment. The seven tracers selected by the LDA were able to explain 91% of the variance and to correctly classify 83% of the source samples. Despite covering less than 10% of the catchment surface area, croplands that replaced the native grasslands supplied the primary sediment source (33%) to the main outlet, followed by subsurface sources (27%). In contrast, native grasslands covering 80% of the surface area provided only 17% of sediment to the river network. These findings confirm that soil erosion processes are accelerating in response to the recent land use changes in the region. To prevent soil loss and sediment delivery to the river systems, land use conversion from native grasslands into croplands should be associated with the implementation of appropriate land conservation practices, such as runoff control, no-tillage system, and crop rotation.

Keywords

Sediment delivery, land use change, soil erosion, sediment source, source-to-sink, conservation farming.

Highlights

- Land use change in the Pampa Biome may increase soil degradation and erosion.
- Croplands provide the main sediment source to the Ibirapuitã river.
- Soil organic matter signatures indicate that croplands are more prone to degradation.
- Introduction of cropland requires appropriate soil conservation measures.
- High contribution of subsurface sources reflects a lack of surface runoff control.

1. Introduction

The Pampa biome (Subtropical Grasslands, Savannas, and Shrublands) in South America has a notably high biodiversity. With an area of approximately 178,800 km² in Brazil (only 2.1% of the total surface of the country; Figure A.1), it is predominantly covered with native grassland (the *Campos Sulinos*), the conservation of which has often been neglected until recent years compared to other biomes in Brazil (Overbeck et al., 2007). The Pampa region receives abundant and intense rainfall occurring on undulated landscapes occupied by soils with a low resistance to water and wind erosion (sandy and shallow soils), which explains why this biome is particularly fragile and vulnerable to degradation (Roesch et al., 2009).

Farmers in the Pampa Biome have been economically motivated to convert native grasslands into croplands due to the increasing profits resulting from crop cultivation over the past 20 years, which are mostly linked to the production of soybeans (Oliveira et al., 2017). Cropland coverage in the Pampa biome of Brazil has expanded by 57% from 2,691 km^2 in 2000/2001 to 4,226 km^2 in 2014/2015 (Silveira et al., 2017), covering 1.5 and 2.4%, respectively, of the biome's total area, respectively (according to the Brazilian Institute of Geography and Statistics - IBGE database). This increase in cropland and cultivated pastureland is closely related to the reduction of native grassland ((MapBiomas, 2019)- Figure A.2). Modernel et al., 2016 observed similar trends in the Pampa region of Argentina and Uruguay, where the conversion of grasslands into cropland and cultivated pastureland (mainly oat and ryegrass) degraded due to overgrazing has increased in response to the higher agricultural commodity prices. Consequently, the conversion of native grasslands into croplands may further increase soil degradation and threaten the ecosystem services provided by the Pampa biome.

The conversion of grasslands into croplands without the implementation of adequate soil management may intensify soil erosion and simultaneously increase the sediment delivery to the river systems (Didoné et al., 2015; Roesch et al., 2009). Accordingly, estimating sediment source contributions is necessary to monitor the respective soil degradation and evaluate the erosion status prevailing under different land uses. The sediment fingerprinting technique has been widely used to quantify the contribution of sediment sources, providing important information about the areas that need more attention for controlling soil erosion (Collins et al., 2020; Walling, 2013). This technique can be implemented with a wide variety of tracers, which should have the capacity to discriminate between potential sediment sources in the catchment of interest and rely on a sound physico-chemical basis (Evrard et al., 2022; García-Comendador et al., 2023).

The soils under native grasslands in the Pampa biome are naturally rich in soil organic matter (SOM) and they have a high potential to store carbon. However, this ecosystem shows a large and rapid loss of soil organic carbon when converted into croplands due to intense soil erosion (Pillar et al., 2012), and it may also alter the SOM composition. Growing crops on these soils is expected to increase SOM mineralization and consequently reduce total organic carbon (TOC) and total nitrogen (TN) contents compared to those found in soils under native grassland (Juracek and Ziegler, 2009). Opposite trends may be observed for N stable isotope ratios ($\delta^{15}N$). The proportion of the heavy isotope ^{15}N in the SOM may increase due to the higher N mineralization caused by soil cultivation and the N enrichment due to fertilizer inputs and/or biological fixation by legumes, such as soybean (Amundson et al., 2003). At the same time, the cultivation of C3 plants (soybean and rice) at the expense of native grasslands predominantly composed of C4 plants may shift their carbon stable isotopes ratios to ^{13}C-

depleted values, providing a potential tracer of sediment origin (Stevenson et al., 2005). Therefore, besides providing potential tracers to discriminate between surface and subsurface sources, parameters related to SOM can also contribute to discriminating areas under degradation from those that are well-managed, since this parameter is directly linked to land use and management (Fox and Papanicolaou, 2007).

The combination of several tracers is recommended to improve discrimination between potential sources (Uber et al., 2019). Fallout radionuclides (^{137}Cs or $^{210}Pb_{xs}$) showed a high potential to discriminate surface and subsurface sources, as their activities are usually significantly higher in topsoil than in subsoil (Evrard et al., 2020). However, their application is limited by the relatively high cost of their measurement and the low availability of low-background analytical facilities increasingly required to analyze them, the relatively large sample quantity required (several grams of material), as well as their limited potential to discriminate between more than two sources. In addition to the information provided by conventional tracers such as radionuclides, geochemical elements and organic matter properties, the use of alternative tracers, based on non-destructive, low-cost, and rapid analyses, may provide useful additional information to improve the overall source discrimination power (Martínez-Carreras et al., 2010a, 2010c). In this regard, colour properties have successfully been used as an alternative tracer in multiple study sites and at various catchment scales (Evrard et al., 2019; Martínez-Carreras et al., 2010b; Pulley et al., 2018; Pulley and Collins, 2021; Ramon et al., 2020; Sellier et al., 2020).

Accordingly, the objective of the current research is to quantify the sediment source contributions, combining organic matter composition, radionuclide, and diffuse reflectance-properties as potential tracers to evaluate the impact of land use change on soil degradation and sediment delivery to the river systems in a catchment representative of the understudied Pampa biome in Southern Brazil.

2. Material and Methods

2.1. Study site

The Ibirapuitã catchment is located in the extreme south of Brazil and is representative of the southern grassland region, typical of the Pampa biome in South America. The outlet of the catchment considered in this study is located next to monitoring point number 76750000 of the Brazilian National Water Agency (ANA, 28°27'22" S, 53°58'24" O) in the municipality of Alegrete, Rio Grande do Sul state (Figure 1). The catchment covers a surface area of approximately 5,943 km². Its altitude ranges between 80 and 370 m a.s.l., and areas above 280 m a.s.l. are located in the headwaters of the catchment, near the border between Brazil and Uruguay. They represent less than 15% of the total catchment surface. Approximately 90% of the catchment is characterised by slopes lower than 15%. Overall, slopes decrease in the northern direction, varying from 2 to 5% in the lower Ibirapuitã region. Land use is dominated by native grasslands (81%) with extensive livestock activities (Figure 2), although soybean crops are increasingly replacing the former native vegetation in the region. The climate is Cfa type according to the Köppen classification, which corresponds to a humid subtropical climate without a defined dry season, with an average precipitation of 1,600 to 1,900 mm per year and an annual average temperature of 17°C (Alvares et al., 2013).

The Ibirapuitã catchment comprises a large heterogeneity of soils, originating from two distinct geological materials, which have a different distribution in three main sub-catchments (Figure 3). The Ibirapuitã – Environmental Protection Area (EPA) subcatchment, is an area controlled by the Chico Mendes Institution of Biodiversity Conservation (ICMBio)

of the Brazilian National Ministry of the Environment since 1992, where native grasslands (85%) and natural forests (10%) dominate. Located in the central portion of the Ibirapuitã catchment, the EPA sub-catchment covers an area of 3,196 km². The main soil types (IUSS Working Group WRB, 2015) are Regosols in the upper half and Acrisols in the lower half, which are set up on basalts of the Serra Geral formation (Fácies Alegrete) and sandstones/silts of the Botucatu formation (Fácies Gramado, Caxias, and Guará), respectively.

The Pai-Passo Stream sub-catchment (PP) covers a surface area of approximately 1,043 km², and it is mainly occupied by native grasslands (83%) with extensive livestock on shallow Regosols developed on basalt (Fácies Alegrete), and paddy fields for irrigated rice production (10%) located in the lower and flatter portions of the landscape, characterized by Planosols and Vertisols.

The Caverá Stream subcatchment (CAV) covers approximately 1,455 km². This is the sub-catchment with the highest percentage of croplands, mostly for rice and soybean production in the summer and for cultivated pastureland in the winter (15%). The native grasslands (73%) have been replaced with croplands mainly on the Acrisols developed on sandstones of the Botucatu formation (Figure 2 and Figure 3).

All sub-catchments share landscape features that concentrate large volumes of runoff on the hillslopes, such as the slope length, flat and undulate reliefs, associated with sandy surface soil layers. These natural characteristics result in their high susceptibility to erosion that is further aggravated by the exposure of the soil through the use of heavy equipment for farming and overgrazing. Furthermore, the absence of riparian zones and the occurrence of preferential paths caused by animal circulation and trampling close to water bodies favour the occurrence of riverbank erosion. These erosion processes are widely observed across the catchment. Although to a lower extent, erosion was also observed on unpaved roads during field campaigns.

2.2. Sediment source sampling

To characterize the potential sediment sources, soil composite samples (n = 132) were taken in representative areas showing evidence of soil erosion and in zones connected to the drainage network. Considered sources included croplands (n = 36), native grasslands (n = 31), unpaved roads (n = 31), and subsurface sources composed of channel bank (n = 18) and gully (n = 16) samples (Figure 2). In the surface sources (i.e., croplands and native grasslands), soil from the upper 0-2 cm layer was collected, as this layer is the most likely to be eroded and transported to the waterways. As for the subsurface sources (i.e., gully and channel bank) and unpaved roads, samples were collected along their exposed faces at sites exposed to erosion. For each composite source sample, around 10 sub-samples were collected within a radius of approximately 50 m, mixed in a bucket, and approximately 500 g of material was stored. Great care was taken to avoid sites that have accumulated sediment originating from other sources, preventing the collection of transient material. The source sampling sites were selected in order to cover all the soil types and the variability in slope positions, as well as the three main tributary catchments. In addition,, the samples were collected in regions with easy access by car. As it corresponds to EPA, access to upper portions of the main catchment was strongly limited due to the absence of accessible roads motorable and dense vegetation in some areas.

2.3. Sediment sampling

Suspended sediment was sampled at the Ibirapuitã catchment outlet and at the confluence with its tributaries following two strategies. The first sampling strategy was the deployment of time-integrating sediment samplers (TISS, *n* = 7) (Figure 2). The sampler designed by (Phillips et al., 2000) consists of a plastic tube of 75 mm in diameter and 80 cm in length, which has a small inlet and outlet tubes (4 mm of diameter) in the extreme edges, allowing suspended sediment to enter and reducing flow velocity to enhance deposition. The equipment is submerged for a certain period in order to cumulate sediment from different rainfall events. The sampling interval was not based on a fixed schedule. Sampling was performed after a minimum time interval of three months and when the river was at a sufficiently low level to have safe access to the samplers. The second strategy was to collect samples of lag deposits after major flooding events when the river discharge exceeded its channel's capacity causing river overflows (*n* = 2).

Three sediment samples were collected at the outlet of the Ibirapuitã catchment, two from TISS (TISS.Out 1 and 2), and one from lag deposits (LD.Out). TISS samples were collected in the tributaries as well: two samples in the Pai-Passo (TISS.PP 1 and 2), two samples in the Ibirapuitã-EPA (TISS.EPA 1 and 2), and one at the Caverá catchment outlet (TISS.Cav). Some TISS samples were lost because the samplers were either flushed away by the flood or likely vandalized. For the sediment samples collected at the main outlet, the first TISS sample covered the winter and early spring periods (from May 25 to October 26, 2018). The second TISS sample covered the spring and summer periods (from October 26, 2018 to February 19, 2019), which coincide with the summer crop cultivation (Figure A.3). Two lag deposit samples were collected, one of them close to the main outlet (LD.Out) and another one close to the EPA catchment outlet (LD.EPA), after the main rainfall-storm event that occurred in January, 2019. Discharge and precipitation data recorded during the suspended sediment sampling time interval are presented in Figure A.3. Rainfall was overall well-distributed throughout the year, with the occurrence of a large rainfall event in January 2019, which resulted in one of the largest flood events of the last 60 years according to the national water agency records (ANA, 2020).

The whole material in LD and TISS samples passed through a 2000 µm mesh sieve, which means that particles larger than this threshold were irrelevant. According to the particle size distribution analyses of suspended sediment samples, more than 80% of the sample volume was composed of particles smaller than 63 µm (Figure A.4). Therefore, we considered that the <63 µm fraction was representative of the suspended sediment samples collected. However, the sandy soils may also provide significant amounts of coarse size sediments that could not be monitored in this study. Further investigations should therefore focus on bed load supply that may contain coarser particles that may be significant in the Ibirapuitã catchment.

2.4. Source and sediment analysis

Samples were oven-dried (45° C), gently disaggregated using a pestle and mortar, and dry-sieved to 63 µm to avoid particle size effects prior to further analysis (Koiter et al., 2013; Laceby et al., 2017). Particle size analyses were carried out on the sediment samples using a LS 13 320 laser diffraction particle size analyser (Beckman Coulter) with a Universal Liquid Module after sieving the samples to 2000 µm.

2.4.1. Total organic matter composition

After further sieving to 63 µm, the samples were hand-ground with a pestle and mortar to obtain a fine and homogeneous powder. Samples were weighted in small tin containers and a tyrosine laboratory standard was inserted for each batch and each four soil or sediment samples to control the reproducibility of the measurements. Total organic carbon (TOC), total nitrogen (TN), $\delta^{13}C$, and $\delta^{15}N$ isotope ratios were measured using continuous flow isotope ratio mass spectrometry (EA-IRMS). Oxygen for combustion was injected for 70 s (30 mL min^{-1}) and temperatures were set at 850 °C and 1120 °C for the reduction and combustion furnaces, respectively (Agnihotri et al., 2014). Analytical precision and repeatability were controlled with tyrosine samples calibrated against international standards (Coplen et al., 1983). In the current research, the mean uncertainties were 0.2‰ for TN, 0.18‰ for TOC, 0.1‰ for $\delta^{13}C$, and 0.2‰ for $\delta^{15}N$. When TN contents were too low, a second run was performed in order to optimize the sample weight for $\delta^{15}N$ measurements, providing enough sample mass for the measurements. Due to the nature of the soil parental material found in the Ibirapuitã catchment (i.e. clayey and siliceous nature), no carbonate removal was required. A selected set of samples (n=8) was analyzed by X-Ray diffraction (Brindley and Brown, 1980), and no carbonate (calcite and dolomite) was found in these samples.

2.4.2. Ultra-violet-visible derived parameters

Thirty parameters were derived from the ultra-violet-visible (UV) diffuse reflectance spectra range (200 to 800 nm, with 1 nm step), measured for each powder sample using a Cary 5000 UV-NIR spectrophotometer (Varian, Palo Alto, CA, USA) at room temperature, using $BaSO_4$ as a 100% reflectance standard. Samples were added into the sample port and care was taken to avoid differences in sample packing and surface smoothness. Twenty-two colour parameters were derived from the UV spectra following the colorimetric models described in detail by (Viscarra Rossel et al., 2006), which are based on the Munsell HVC, RGB, the decorrelation of RGB data, CIELAB, and CIELUV Cartesian coordinate systems, three derived from the Hunterlab colour space model (HunterLab, 2015) and two-color indices (Pulley et al., 2018). Finally, 27 colour metric parameters were derived from the spectra of source and sediment samples and used as potential tracers (L, L*, a, a*, b, b*, C*, h, RI, x, y, z, u*, v*, u', v', Hvc, hVc, hvC, R, G, B, HRGB, IRGB, SRGB, CI, and SI) (Viscarra Rossel et al., 2006). Three additional parameters were calculated from the second derivative curves of remission functions in the visible range of sediment sources and sediment samples, which displayed three major absorption bands at short wavelengths commonly assigned to Fe-oxides (Caner et al., 2011; Fritsch et al., 2005). The first band (A1) corresponds to the single electron transition of goethite (Gt), whereas the two others correspond to the electron pair transition for goethite (A2) and for hematite (Hm) (A3). More details about the calculation of UV-derived parameters can be found in (Ramon et al., 2020).

2.4.3. Fallout radionuclides analysis

Fallout radionuclide activities (^{137}Cs and ^{210}Pb) were measured by gamma spectrometry using low-background high-purity germanium detectors (Canberra/Ortec). Between 10 to 20 g of samples were weighted into polyethylene containers, sealed airtight, and analysed on a detector installed in a lead-protected shield. Measurements were conducted between 80 x 10^5 – 130 x 10^5 s to optimise counting statistics. The fallout radionuclides ^{210}Pb and ^{137}Cs were obtained from the counts at 46.5 keV and 661.6 keV, respectively. The unsupported or excess lead-210 ($^{210}Pb_{xs}$) was calculated by subtracting the

supported activity from the total ^{210}Pb activity using two ^{238}U daughters, i.e. ^{214}Pb (average count at 295.2 and 351.9 keV) and ^{214}Bi (609.3 keV). Radionuclide activities were decay-corrected to the sampling date (October 8th, 2018). For samples with ^{137}Cs activities lower than the detection limits, they were attributed activity values amounting to half of the detection limit reached for these samples.

2.4.4. Sediment source discrimination and apportionment

Some potential tracers presented a large variability within the same source sediment group. Therefore, the samples presenting values for more than three parameters outside of the range defined by the mean ±2 standard deviations of the given parameter were considered outliers and removed from further analysis (Pulley et al., 2020).

After this first step, the tracer selection followed the classical three-step procedure: (i) a range test, (ii) a Kruskal-Wallis *H* test (KW *H* test), and (iii) a linear discriminant function analysis (LDA). For passing the range test, mean parameters values for sediment must fall within the range between the maximum and minimum values observed for the sources. The KW *H* test was then performed to test the null hypothesis ($p < 0.05$) that the sources belong to the same population. The variables that provided significant discrimination between the sources sediment were analysed with a forward stepwise LDA ($p < 0.1$) in order to reduce the number of variables to a minimum that maximizes source discrimination (Collins et al., 2010). The statistical analyses were performed with R software (R Development Core Team, 2017) and more details on the procedure can be found in (Batista et al., 2018).

The source contributions were estimated by minimizing the sum of squared residuals (SSR) of the following mass balance un-mixing model:

$$SSR = \sum_{i=1}^{n} \left(\left(C_i - \left(\sum_{s=1}^{m} P_s S_{si} \right) \right) \Big/ C_i \right)^2 \quad (1)$$

where n is the number of variables/elements used for modelling, C_i is the value of the parameter i in the target sediment, m is the number of sources, P_s is the optimized relative contribution of source s by SSR minimizing function, and S_{si} is the concentration of element i in the source s.

Optimization constraints were set to ensure that source contributions were non-negative and that their sum equalled 1. The un-mixing model was solved by a Monte Carlo simulation with 2500 iterations. More information about model settings and compilation can be found in (Batista et al., 2018). Model uncertainties were evaluated based on the interquartile variation range of the predictions from the multiple iterations of Monte Carlo simulation. The median and interquartile ranges are presented as the source contribution for each of the target sediment samples modelled.

3. Results

3.1. Source and sediment properties

3.1.1. Organic matter composition

The four parameters related to the organic matter composition showed a significant difference between at least two sources (p <0.05) (Table 1). Total organic C (TOC) and total N (TN) were highly correlated (R^2 = 0.97) with a mean TOC/TN ratio of 10.3, and their

concentration in the sources and sediments showed similar patterns (Figure A.6). Mean TOC and TN contents were higher in the native grasslands compared to the other sources. However, they showed a high standard deviation (SD) (46.2 ±16.1 g kg^{-1} and 4.5 ±1.5 g kg^{-1}, respectively) (Figure 4). Unpaved roads and subsurface sources had much lower TOC (5.0 ±1.9 g kg^{-1} and 14.5 ±7.6 g kg^{-1}, respectively) and TN contents (0.6 ±0.3 g kg^{-1} and 1.3 ±0.6 g kg^{-1}, respectively), with lower SDs. Croplands had lower TOC and TN contents (32.7 g kg^{-1} and 3.3 g kg^{-1}, respectively) than native grasslands, with values closer to those observed in sediment samples (23.5 ± 4.5 g kg^{-1} and 2.2 ± 0.5 g kg^{-1}, respectively).

The results indicate that TOC and TN can provide good discrimination between surface (croplands and native grasslands) and subsurface (unpaved roads, erosion channel, and channel bank) sources (Figure 4). Furthermore, the mean percentage of TOC and TN in native grassland is higher than under croplands, and this difference can be useful to quantify the contribution of cropland areas to the sediment collected in the river (Table 1). TOC and TN contents in sediment samples fall within the range of values found in potential sources, fulfilling one of the fundamental principles of sediment fingerprinting, according to which the potential tracers must be conservative (Smith and Blake, 2014).

The $\delta^{13}C$ and $\delta^{15}N$ values showed contrasting signatures between potential sediment sources, mainly between subsurface sources and croplands. Croplands showed more negative mean values with high SD (-19.0 ±2.0 ‰), while subsurface sources showed less negative mean $\delta^{13}C$ value (-17.2 ±2.3 ‰) (Table 1). The $\delta^{15}N$ presented higher mean values in croplands (8.1 ±1.0 ‰) and lower values in the native grasslands source (7.1 ±1.3 ‰), while unpaved roads and subsurface sources showed intermediate values (7.9 ±0.9 ‰ and 7.4 ±0.9 ‰, respectively). For 27 samples including five sediment samples, the TN concentration was too low to allow accurate $\delta^{15}N$ measurements. Because of the limited number of sediment samples for which $\delta^{15}N$ data was available and because of the high difference of $\delta^{13}C$ values between sediment and source samples (Figure 4), the isotopes were not included in the sediment fingerprinting approach as potential tracers.

3.1.2. Fallout radionuclide activities

Fallout radionuclide activity was sufficiently high to be determined in all the analysed samples. For both fallout radionuclides of interest in the present study, i.e. ^{137}Cs and $^{210}Pb_{xs}$, the mean activities were higher in the native grasslands (3.4 ± 1.6 Bq kg^{-1} and 197.7 ± 101.3 Bq kg^{-1}, respectively) than in croplands (2.7 ± 1.2 Bq kg^{-1} and 136.7 ± 63.5 Bq kg^{-1}, respectively) (Figure 5). However, the variability of values within each superficial source was very high, compared to the more uniform results observed for the subsurface sources (Figure A.6).

3.1.3. UV derived parameters

Ultra-violet-visible derived parameters showed a large variation within sources, while sediment sample values remained very homogeneous (Figure 6). Although many parameters could be extracted from these analyses, only a couple of them turned out to be useful to characterize different sources. Most of the UV-derived parameters are highly correlated with each other and are grouped in the same cluster, explaining the same variance observed between sediment sources (Figure A.5).

Parameters related to the iron oxides, such as A1, A2, and A3, showed no significant differences between surface sources (Table 1). These tracers are more related to parental material, soil types, and formation. Consequently, values differ mainly between surface and subsurface sources, as can be observed for A1, with mean values of 0.0008465 and 0.001188,

respectively (Figure 6). Colour parameters such as chroma and value are influenced by the carbon content and land use type (Wills et al., 2007). Luminosity index (L*), which is related to the dark or light colour of the soil (Hunter Laboratories, 1996), has lower values for native grasslands (48.6 ±5.8) in relation to croplands (52.3 ±3.2) (where a low number (0-50) indicates dark and a high number (50-100) indicates light colours). This difference may be attributed to the difference in TOC, which is one of the main properties responsible for changing soil colours (Viscarra Rossel et al., 2006). In contrast, RI values were almost twice higher in the native grasslands (0.81 ±0.6) than in the other three sources (mean of 0.47), and it is one of the parameters that presents the lowest correlation with the other parameters evaluated (Figure A.5). A significant difference is observed between the subsurface source and unpaved roads for the hue (h) value of CIE and chroma (hvC) of the Munsell chart. Lower chroma values decrease when soil is saturated and chemically reduced, and these lower values can be observed in subsurface sources (gully and channel bank) (Sánchez-Marañón, 2011).

3.2. Selection of sediment tracers

In the first step of the data analysis, 15 source samples were removed because more than three parameters fell outside of the range based on the mean of the respective group and two standard deviations (SD). Therefore, only 117 source samples were kept for subsequent analyses. In this study, $\delta^{15}N$ was not used as a tracer, because in several sources (n = 22) and sediment (n = 5) samples, the TN concentration was too low to get accurate isotopic measurements, although exhibiting a conservative behaviour and a potential discrimination power between sources. From the 34 parameters considered as potential tracers, only 14 were conservative, with the sediment values lying between the mean of the sources ± 1 SD. According to the KW H-test, all parameters hold the potential to discriminate between at least two sources, allowing all 14 conservative parameters to enter the linear discriminant analysis (LDA).

Among the 14 parameters, seven were selected by LDA as the optimal set of tracers (Table 2). TN, h, $^{210}Pb_{xs}$, A1, hvC, RI, and L were able to explain 91.1% of the variance between source samples (Table 2). The LDA bi-plots presented in Figure 7 demonstrate the source reclassification using the best set of tracers from the statistical analysis. Discrimination between surface and subsurface sources was very clear. The mean Square Mahalanobis distance between the surface and subsurface source was 18.5; 11.6 for croplands, and 25.5 for native grasslands (Table 2). The Square Mahalanobis distance between croplands and native grasslands was very low (4.5), but it was still significant ($p<0.01$). The same was observed between subsurface sources (channel bank and gully) and unpaved roads (5.3, $p<0.01$). On average, 83% of the source samples were correctly classified by the LDA.

3.3. Sediment source apportionment

During the first period of sediments sampled using the time-integrating sediment samplers (TISS), the mixing model results indicate croplands as the main sediment source in all sediment samples collected from the Ibirapuitã River (Figure A.7). The Caverá and Pai-Passo sub-catchment showed a higher proportion of sediment from croplands (41% and 40%, respectively) compared to the other two catchments (Figure 8). The Caverá catchment also had the highest contribution of sediment from native grasslands (32%), while in the other sites this contribution ranged between 18% and 20%. Subsurface and unpaved road contributions were the least important for both catchments in the first period. For the Caverá

catchment, subsurface and unpaved roads correspond to only 27% of the total sediment supply to the river, while for the sub-catchments Environmental Protection Area (EPA), Pai-Passo, and in the Ibirapuitã catchment outlet they represent 47%, 41%, and 41%, respectively (Figure 8).

For the second period of TISS sampling, a higher contribution from subsurface and unpaved roads was observed (Figure A.7), except in the Caverá sub-catchment in which the sediment sample was lost. Altogether, subsurface and unpaved roads supplied more than 60% of sediment. Native grassland's contribution ranged between 9% and 13%, while the mean contribution of croplands was 27% for the EPA sub-catchment, Pai-Passo sub-catchment, and the main outlet of the Ibirapuitã River catchment. The source contribution observed for the second TISS period was very similar to the source contribution observed for the sediment samples of lag deposits (LD). These samples were collected just after the large rainfall event that occurred in January 2019, which could be responsible to a large extent for the sediment transport that occurred during the entire second period.

4. Discussion

4.1. Source and sediment samples composition

The Ibirapuitã River catchment shows a high diversity of soil types, mainly due to the different geological basements and landscape variability found in the region. In addition, the differences in land use management may result in such a high intra-source variation as that observed for the parameters evaluated in the current research, especially in surface sources. Native grassland was the source showing the greater variability, mainly for parameters related to TOC and fallout radionuclide activities. Overgrazing in fragile areas has likely resulted in native grassland degradation due to the higher soil exposure to water erosion, including the formation of gullies (Cordeiro and Hasenack, 2009). Furthermore, the high variability of native grassland management operations (e.g., different fertilization, stoking rate, etc) by farmers can likely explain this high intra-source variability.

Grasslands represent a significant sink of carbon, and according to the meta-analysis conducted by (Guo and Gifford, 2002), 59% of the soil organic carbon is lost when grasslands are converted into croplands. This can explain the lower TOC and TN content found in croplands compared to grasslands in the investigated catchment. The conversion of native grasslands into croplands can result in a fast depletion of soil organic matter (SOM), as a consequence of a negative balance between C inputs by plant and microorganism residues and C losses as CO_2 due to microbial oxidation of SOM. At the same time, SOM is more concentrated in the soil surface layers, which are the most exposed to soil erosion. When the soil is plowed for crop cultivation, the soil is further exposed to the impact of rainfall, breaking the soil aggregates and exposing the physically protected SOM. Accordingly, the erosion processes accelerate the mineralization of SOM into atmospheric CO_2 and also make the C bound to sediment to be potentially transported to water courses (Lal, 2003). Beyond the impacts on soil degradation, (Booman et al., 2012) observed that the reduction of grassland area in the Argentinian Pampa result in a drastic modification of the catchment hydrological behaviour.

The SOM was found to be more depleted in ^{13}C in cropland samples compared to native grassland samples, suggesting that the introduction of C3 plants may be currently changing the C signature of the SOM. In the *Campos Sulinos* of the Pampa biome, the C4 grasslands dominate, resulting in a greater accumulation of ^{13}C in the soil ((Andrade et al., 2019). The conversion of native grasslands into croplands with C3 plants, mainly soybean

(*Glycine max*) and rice (*Oriza sativa*), tends to reduce the proportion of ^{13}C, which results in more negative values of $\delta^{13}C$. In addition, during the winter, these areas are also usually cultivated with C3 grass pastures, such as ryegrass (*Lolium multiflorum*) and oat (*Avena sativa*).

The higher $\delta^{15}N$ values in cropland and the decrease of TN can be related to the selective mineralization of SOM, leading to TN depletion by leaching or volatilization and ^{15}N enrichment in the remaining soil organic matter (Xu et al., 2010). Moreover, plants tend to favour the incorporation of the light N isotope ^{14}N over ^{15}N. Accordingly, the plant tissues are usually depleted in ^{15}N and the N remaining in the soil is enriched in ^{15}N (Fox and Papanicolaou, 2008). The opposite behaviour is observed in native grasslands, as the highest TN content and lower losses of N by mineralization processes result in lower $\delta^{15}N$. At the same time, the plant residues deposited on the soil surface and depleted in ^{15}N, result in lower $\delta^{15}N$ in the soil surface compared to the subsurface sources (Huon et al., 2017). The temporal stability of TOC and TN in the fine suspended sediment generated by water erosion makes the measurement of these variables usable as an alternative tracer for quantifying sediment source contributions (i.e., using end-member mixing models) (Huon et al., 2013; Riddle et al., 2022).

Ultra-violet-visible derived parameters are mainly controlled by the carbon content and variables related to the pedogenesis process, such as iron oxide and clay content (Bayer et al., 2012). The current land use-based approach did not take into account the soil type variability, which is particularly high in the Ibirapuitã catchment. The high variability of these parameters within sources can be explained by this soil-type variability. As a consequence, most colour parameters, and those related to iron oxides, were not selected as tracers to discriminate between land-use-based sources.

The variability of radionuclide activities in surface sources can be related to the soil degradation and erosion status of each sampled site (Evrard et al., 2020). The soil degradation status was not taken into account during the sampling campaign, where a wide variability of soil management conditions was covered within each land use. This variability was not observed in subsurface sources, which were sheltered from atmospheric fallout. The lower mean activity of ^{137}Cs and $^{210}Pb_{xs}$ observed in croplands compared to native grasslands can be indicative of the higher soil erosion rates occurring under croplands, confirming what was deduced from the observations made on the SOM composition parameters. As for croplands, some native grassland samples were depleted in ^{137}Cs and also in $^{210}Pb_{xs}$, suggesting that the surface soil layer with higher radionuclide activities was removed by soil erosion.

4.2. Sediment source contribution

The mixing model results indicate that land use management can play an important role in controlling sediment delivery to the river. The combination of soils highly sensitive to erosion, a high rainfall erosivity (Almagro et al., 2017), steep slopes, and inappropriate land use and management (Roesch et al., 2009) may increase connectivity across catchments during different periods (Ares et al., 2020) accelerating the transfer of sediments to the river. The first period covered by TISS samples represents the time after the harvesting of summer crops (rice and soybean mainly) when the soil is exposed to rainfall without cover crops. During this first period, croplands supplied the main source of suspended sediment. It should be noted that the proportion of the catchment area occupied by croplands remains very low nowadays, covering only 10% of the total catchment surface. Besides that, samples from the sub-catchments, that showed higher proportions of croplands, such as Caverá and Pai-Passo,

displayed a slightly higher contribution of sediment originating from croplands. Croplands and pastures have already been reported as the main sediment sources in other sediment tracing studies developed in southern Brazil (Tiecher et al., 2018, 2017) where high erosion rates and sediment yields were quantified (Didoné et al., 2014).

In the first sampling period, the higher contribution of native grasslands in the Caverá sub-catchment compared to the other sub-catchments (Figure 8) is probably due to the geological basement of the Caverá sub-catchment, which is mainly composed of sandstone (Figure 3). This type rock generates sandy soils that are more sensitive to erosion (Costa et al., 2018) and, consequently, to degradation brought on by poor land management. The main threats to the Pampa biome ecosystems have already been identified as overgrazing and eventual burning of native grasslands, especially on sand-textured soils, followed by erosion and sandification (Roesch et al., 2009). The continued expansion of agriculture in the Pampa region may further increase the contribution of sediments and contaminants to the river network due to soil degradation. The region has a high potential for nutrients and contaminants losses due to soil erosion. A global estimation of P losses due to soil erosion showed that, in this region, the P losses can be in the order of 1.1 to 20.0 kg ha-1 yr-1 (Alewell et al., 2020). Appropriate soil conservation practices have to be implemented to avoid the situation where soil degradation can lead to an irreversible status of sandification (Roesch et al., 2009).

The high rainfall-runoff event that took place in January 2019 is likely the reason for the increased contribution of sediments from subsurface sources during the second phase of sediment sampling utilizing TISS. The overflow of the river exacerbated the erosion of channels and gullies, increasing their contribution to sediment. For the sediment sampled in the lag deposits, similar source contributions were calculated as for the TISS samples during this second period. Previous studies evaluating the sediment source contributions in paired catchments of the Pampa biome, one with two nested forest plantations (Rodrigues et al., 2018) and the other with paired catchments under forest plantation and native grasslands (Valente et al., 2020), outlined in a similar way that stream banks provided the main sediment source through the collapse of river banks. The absence of riparian vegetation and the occurrence of outcropping deep sandy soil profiles are widely observed in the Ibirapuitã catchment, which may promote bank erosion. Additionally, it was shown that overgrazed fields with cattle having unrestricted access to stream channels accelerated erosion of stream banks and gullies (Zaimes et al., 2019). Moreover, the long and undulating slopes observed in this region facilitate the runoff concentration in the convergence zones, leading to the formation of gullies. Furthermore, Valente et al. (2020) also showed that grasslands with intensive livestock farming are counterintuitively more sensitive to soil erosion than forest plantations in the Pampa biome.

Overall, the current research results showed that land use change consisting of the conversion of native grasslands into croplands may lead to several deleterious environmental impacts. As observed by Foucher et al. (2023), in the nearby Rio Negro catchment in Uruguay, the conversion of native grasslands in the Pampa Biome into areas for grain cultivation or planted forests, without the implementation of appropriate soil management practices, result in an increase in erosion rates and sediment input into river systems and dam reservoirs. As a result, better management practices have to be promoted under native grasslands to reduce overland flow and subsequent gully and stream bank erosion in lower landscape areas. Grasslands show a high potential to capture and store carbon in the soil (Viglizzo et al., 2019) and the grasslands of the Pampa biome provide important ecosystem

services. Their protection requires strategies to improve the land management (Modernel et al., 2016). As already pointed out by (Oliveira et al., 2017), more studies are needed to give support for policymakers to define the best strategies for achieving the Pampa biome grasslands conservation.

4.3. Limitations of the study

Tracing sediment sources in catchments of this size and with these characteristics poses numerous challenges. Among them, we can mention: 1) the difficulty in obtaining samples to characterize sources with a spatial distribution covering the entire catchment. Due to the low population density in the region and the occurrence of an EPA in its upper parts, road access is quite limited. Furthermore, as it is a very remote region, it was not possible to identify landowners before accessing their properties, so that for safety reasons, some areas could not be accessed; 2) in ideal conditions, more sediment samples should have been collected covering a greater spatial and temporal variability of river flow conditions. Some of the sediment samplers installed in the rivers were washed away during floods, and some of them were also removed by local people. An assessment of the contribution of sub-catchments could also help to better understand the temporal and regional variations in sediment source contributions; 3) for this particular catchment, greater attention should be given to sediments with a particle size greater than 63 µm. Since the soils in this area have a high sand content, this coarser material also contributes substantially to the total sediment flux. The difficulty is to identify appropriate tracers to investigate the contribution of this coarser material, which is challenging as this fraction is depleted in most tracers found enriched in the finer fraction and used to trace its contribution.

5. Conclusions

This study provided some of the first insights into the impacts of recent land use changes on sediment sources supplied to the water bodies in a representative catchment of the Brazilian Pampa biome. Croplands (33%) and subsurface sources (27%) were shown to supply the main sediment sources in the Ibirapuitã river catchment, followed by unpaved roads (24%). Subsurface sources were the main sources of lag deposit while croplands were the main source of suspended sediment. However, the high cropland contribution to sediments (33%) is raising concerns as it currently only covers 10% of the total catchment area and it already provides a disproportionate contribution of material to river systems. This demonstrates that erosion processes have intensified in this region following the conversion of native grasslands into croplands. Croplands are probably exposed to more severe soil degradation, as evidenced by the discrepancies between the soil signatures under croplands and native grasslands in terms of the organic matter composition and radionuclide activity. Accordingly, the conversion of native grasslands into farming areas, in the current conditions of soil management, tends to reduce the soil contents in soil organic carbon, decreasing soil quality, and increasing the degradation of water resources through the accelerated transfer of sediments and potentially associated contaminants. Furthermore, we observed that extreme rainfall-runoff events can have a significant impact on the sediment dynamics of the catchment, and considering their increased frequency due to climate change, it is necessary to adopt measures to mitigate their impacts. In order to achieve a sustainable agricultural development in this region, it is crucial to implement appropriate soil conservation practices

since the current management appears clearly to be insufficient to control the transfer of sediments from cropland to the river system.

Acknowledgements

Funding: The authors are grateful to National Council for Scientific and Technological Development – CNPq and Coordination for the Improvement of Higher Education Personnel – CAPES for providing financial support. Furthermore, the authors are also grateful to CAPES for founding the PhD scholarship of the first author Rafael Ramon in the framework of the CAPES-COFECUB Project [No. 88887.196234/2018-00]. We are grateful to the Nexus Bioma Pampa project sponsored by the CNPq call MCTI/CNPq Nº 20/2017, in the person of its coordinator Vicente Celestino Pires Silveira, who financed part of this project. We are also grateful to the FUNDAÇÃO DE ESTUDOS AGRÁRIOS LUIZ DE QUEIROZ – FEALQ, AGRISUS PROCESS N° 2920/20, for providing financial support.

The authors are also grateful to J. Patrick Laceby for earlier contributions to this work and for providing access to his R modelling code. Irène Lefèvre is also gratefully acknowledged for conducting the gamma spectrometry analyses.

6. References

Agnihotri, R., Kumar, R., Prasad, M.V.S.N., Sharma, C., Bhatia, S.K., Arya, B.C., 2014. Experimental Setup and Standardization of a Continuous Flow Stable Isotope Mass Spectrometer for Measuring Stable Isotopes of Carbon, Nitrogen and Sulfur in Environmental Samples. MAPAN 29, 195–205. https://doi.org/10.1007/s12647-014-0099-8

Alewell, C., Ringeval, B., Ballabio, C., Robinson, D.A., Panagos, P., Borrelli, P., 2020. Global phosphorus shortage will be aggravated by soil erosion. Nat Commun 11. https://doi.org/10.1038/s41467-020-18326-7

Almagro, A., Oliveira, P.T.S., Nearing, M.A., Hagemann, S., 2017. Projected climate change impacts in rainfall erosivity over Brazil. Sci Rep 7, 8130. https://doi.org/10.1038/s41598-017-08298-y

Alvares, C.A., Stape, J.L., Sentelhas, P.C., de Moraes Gonçalves, J.L., Sparovek, G., 2013. Köppen's climate classification map for Brazil. Meteorologische Zeitschrift 22, 711–728. https://doi.org/10.1127/0941-2948/2013/0507

Amundson, R., Austin, A.T., Schuur, E.A.G., Yoo, K., Matzek, V., Kendall, C., Uebersax, A., Brenner, D., Baisden, W.T., 2003. Global patterns of the isotopic composition of soil and plant nitrogen. Global Biogeochem Cycles 17. https://doi.org/10.1029/2002GB001903

ANA, N.W.A., 2020. HidroWeb: hydrologycal information system. [WWW Document]. URL http://www.snirh.gov.br/hidroweb/serieshistoricas (accessed 9.5.20).

Andrade, B.O., Bonilha, C.L., Overbeck, G.E., Vélez-Martin, E., Rolim, R.G., Bordignon, S.A.L., Schneider, A.A., Vogel Ely, C., Lucas, D.B., Garcia, É.N., dos Santos, E.D., Torchelsen, F.P., Vieira, M.S., Silva Filho, P.J.S., Ferreira, P.M.A., Trevisan, R., Hollas, R., Campestrini, S., Pillar, V.D., Boldrini, I.I., 2019. Classification of South Brazilian grasslands: Implications for conservation. Appl Veg Sci 22, 168–184. https://doi.org/10.1111/avsc.12413

Ares, M.G., Varni, M., Chagas, C., 2020. Runoff response of a small agricultural basin in the argentine Pampas considering connectivity aspects. Hydrol Process 34, 3102–3119. https://doi.org/10.1002/hyp.13782

Batista, P.V.G., Laceby, J.P., Silva, M.L.N., Tassinari, D., Bispo, D.F.A., Curi, N., Davies, J., Quinton, J.N., 2018. Using pedological knowledge to improve sediment source apportionment in tropical environments. J Soils Sediments. https://doi.org/10.1007/s11368-018-2199-5

Bayer, A., Bachmann, M., Müller, A., Kaufmann, H., 2012. A Comparison of Feature-Based MLR and PLS Regression Techniques for the Prediction of Three Soil Constituents in a Degraded South African Ecosystem. Appl Environ Soil Sci 2012, 1–20. https://doi.org/10.1155/2012/971252

Booman, G.C., Calandroni, M., Laterra, P., Cabria, F., Iribarne, O., Vázquez, P., 2012. Areal changes of lentic water bodies within an agricultural basin of the Argentinean Pampas. Disentangling land management from climatic causes. Environ Manage 50, 1058–1067. https://doi.org/10.1007/s00267-012-9943-1

Brindley, G.W., Brown, G. (Eds.), 1980. Crystal Structures of Clay Minerals and their X-Ray Identification. Mineralogical Society of Great Britain and Ireland, Colchester and London. https://doi.org/10.1180/mono-5

Caner, L., Petit, S., Joussein, E., Fritsch, E., Herbillon, A.J., 2011. Accumulation of organo-metallic complexes in laterites and the formation of Aluandic Andosols in the Nilgiri Hills (southern India): similarities and differences with Umbric Podzols. Eur J Soil Sci 62, 754–764. https://doi.org/10.1111/j.1365-2389.2011.01389.x

Collins, A.L., Blackwell, M., Boeckx, P., Chivers, C.A., Emelko, M., Evrard, O., Foster, I., Gellis, A., Gholami, H., Granger, S., Harris, P., Horowitz, A.J., Laceby, J.P., Martinez-Carreras, N., Minella, J.P.G., Mol, L., Nosrati, K., Pulley, S., Silins, U., da Silva, Y.J., Stone, M., Tiecher, T., Upadhayay, H.R., Zhang, Y., 2020. Sediment source fingerprinting: benchmarking recent outputs, remaining challenges and emerging themes, Journal of Soils and Sediments. Journal of Soils and Sediments. https://doi.org/10.1007/s11368-020-02755-4

Collins, A.L., Zhang, Y., Walling, D.E., 2010. Apportioning sediment sources in a grassland dominated agricultural catchment in the UK using a new tracing framework. Sediment Dynamics for a Changing Future 337, 68–75.

Coplen, T.B., Kendall, C., Hopple, J., 1983. Comparison of stable isotope reference samples. Nature 302, 236–238.

Cordeiro, J.L.P., Hasenack, H., 2009. Cobertura vegetal atual do Rio Grande do Sul, in: Pillar, V.D., Muller, S.C., Castilhos, Z.M. de S., Jacques, A.V.Á. (Eds.), Campos Sulinos - Conservação e Uso Sustentável Da Biodiversidade. MMA, Brasília, pp. 285–299.

Costa, C.W., Lorandi, R., de Lollo, J.A., Imani, M., Dupas, F.A., 2018. Surface runoff and accelerated erosion in a peri-urban wellhead area in southeastern Brazil. Environ Earth Sci 77, 1–18. https://doi.org/10.1007/s12665-018-7366-x

Didoné, E.J., Minella, J.P.G., Merten, G.H., 2015. Quantifying soil erosion and sediment yield in a catchment in southern Brazil and implications for land conservation. J Soils Sediments 15, 2334–2346. https://doi.org/10.1007/s11368-015-1160-0

Didoné, E.J., Minella, J.P.G., Reichert, J.M., Merten, G.H., Dalbianco, L., de Barrros, C.A.P., Ramon, R., 2014. Impact of no-tillage agricultural systems on sediment yield in two large catchments in Southern Brazil. J Soils Sediments 14, 1287–1297. https://doi.org/10.1007/s11368-013-0844-6

Evrard, O., Batista, P.V.G., Company, J., Dabrin, A., Foucher, A., Frankl, A., García-Comendador, J., Huguet, A., Lake, N., Lizaga, I., MartínezCarreras, N., Navratil, O., Pignol, C., Sellier, V., 2022. Improving the design and implementation of sediment fingerprinting studies: summary and outcomes of the TRACING 2021 Scientific School. J Soils Sediments 22, 1648–1661. https://doi.org/10.1007/s11368-022-03203-1

Evrard, O., Chaboche, P.-A., Ramon, R., Foucher, A., Laceby, J.P., 2020. A global review of sediment source fingerprinting research incorporating fallout radiocesium (137Cs). Geomorphology 362, 107103. https://doi.org/10.1016/j.geomorph.2020.107103

Evrard, O., Durand, R., Foucher, A., Tiecher, T., Sellier, V., Onda, Y., Lefèvre, I., Cerdan, O., Laceby, J.P., 2019. Using spectrocolourimetry to trace sediment source dynamics in coastal catchments draining the main Fukushima radioactive pollution plume (2011–2017). J Soils Sediments 19, 3290–3301. https://doi.org/10.1007/s11368-019-02302-w

Foucher, A., Tassano, M., Chaboche, PA., Chalar, G., Cabrera, M., Gonzalez, J., Cabral, P., Simon, A., Agelou, M., Ramon, R., Tiecher, T., Evrard, O.. Inexorable land degradation due to agriculture expansion in South American Pampa. Nat Sustain 6, 662–670 (2023). https://doi.org/10.1038/s41893-023-01074-z

Fox, J.F., Papanicolaou, A.N., 2008. Application of the spatial distribution of nitrogen stable isotopes for sediment tracing at the watershed scale. J Hydrol (Amst) 358, 46–55. https://doi.org/10.1016/j.jhydrol.2008.05.032

Fox, J.F., Papanicolaou, A.N., 2007. The use of carbon and nitrogen isotopes to study watershed erosion processes. J Am Water Resour Assoc 43, 1047–1064. https://doi.org/10.1111/j.1752-1688.2007.00087.x

Fritsch, E., Morin, G., Bedidi, A., Bonnin, D., Balan, E., Caquineau, S., Calas, G., 2005. Transformation of haematite and Al-poor goethite to Al-rich goethite and associated yellowing in a ferralitic clay soil profile of the middle Amazon Basin (Manaus, Brazil). Eur J Soil Sci 56, 575–588. https://doi.org/10.1111/j.1365-2389.2005.00693.x

García-Comendador, J., Martínez-Carreras, N., Fortesa, J., Company, J., Borràs, A., Palacio, E., Estrany, J., 2023. In-channel alterations of soil properties used as tracers in sediment fingerprinting studies. Catena (Amst) 225, 107036. https://doi.org/10.1016/J.CATENA.2023.107036

Guo, L.B., Gifford, R.M., 2002. Soil carbon stocks and land use change : a meta analysis. Glob Chang Biol 345–360. https://doi.org/10.1046/j.1354-1013.2002.00486.x

Hunter Laboratories, 1996. Insight on Color: Hunter Lab Color Scale. Applications Note 8, 1–4.

HunterLab, 2015. The basics of color perception and measurement [WWW Document]. URL https://www.hunterlab.com/basics-of-color-theory.pdf?r=false (accessed 7.9.19).

Huon, S., de Rouw, A., Bonté, P., Robain, H., Valentin, C., Lefèvre, I., Girardin, C., Le Troquer, Y., Podwojewski, P., Sengtaheuanghoung, O., 2013. Long-term soil carbon loss and accumulation in a catchment following the conversion of forest to arable land in northern Laos. Agric Ecosyst Environ 169, 43–57. https://doi.org/10.1016/j.agee.2013.02.007

Huon, S., Evrard, O., Gourdin, E., Lefèvre, I., Bariac, T., Reyss, J., Henry des Tureaux, T., Sengtaheuanghoung, O., Ayrault, S., Ribolzi, O., 2017. Suspended sediment source and propagation during monsoon events across nested sub-catchments with contrasted land uses in Laos. J Hydrol Reg Stud 9, 69–84. https://doi.org/10.1016/j.ejrh.2016.11.018

IUSS Working Group WRB, 2015. World reference base for soil resources 2014, update 2015 International soil classification system for naming soils and creating legends for soil maps. World Soil Resources Reports No. 106. FAO, Rome.

Juracek, K.E., Ziegler, A.C., 2009. Estimation of sediment sources using selected chemical tracers in the Perry lake basin, Kansas, USA. International Journal of Sediment Research 24, 108–125. https://doi.org/10.1016/S1001-6279(09)60020-2

Koiter, A.J., Owens, P.N., Petticrew, E.L., Lobb, D.A., 2013. The behavioural characteristics of sediment properties and their implications for sediment fingerprinting as an approach for identifying sediment sources in river basins. Earth Sci Rev 125, 24–42. https://doi.org/10.1016/j.earscirev.2013.05.009

Laceby, J.P., Evrard, O., Smith, H.G., Blake, W.H., Olley, J.M., Minella, J.P.G., Owens, P.N., 2017. The challenges and opportunities of addressing particle size effects in sediment source fingerprinting: A review. Earth Sci Rev 169, 85–103. https://doi.org/10.1016/j.earscirev.2017.04.009

Lal, R., 2003. Soil erosion and the global carbon budget. Environ Int 29, 437–450. https://doi.org/10.1016/S0160-4120(02)00192-7

MapBiomas, 2019. Projeto MapBiomas – Coleção v4.0 da Série Anual de Mapas de Cobertura e Uso de Solo do Brasil [WWW Document]. Projeto MapBiomas - é uma iniciativa multi-institucional para gerar mapas anuais de cobertura e uso do solo a partir de processos de classificação automática aplicada a imagens de satélite. A descrição completa do projeto encontra-se em http://mapbiomas.o. URL http://mapbiomas.org (accessed 6.2.19).

Martínez-Carreras, N., Krein, A., Gallart, F., Iffly, J.F., Pfister, L., Hoffmann, L., Owens, P.N., 2010a. Assessment of different colour parameters for discriminating potential suspended sediment sources and provenance: A multi-scale study in Luxembourg. Geomorphology 118, 118–129. https://doi.org/10.1016/j.geomorph.2009.12.013

Martínez-Carreras, N., Krein, A., Gallart, F., Iffly, J.F., Pfister, L., Hoffmann, L., Owens, P.N., 2010b. Assessment of different colour parameters for discriminating potential suspended sediment sources and provenance: A multi-scale study in Luxembourg. Geomorphology 118, 118–129. https://doi.org/10.1016/j.geomorph.2009.12.013
Martínez-Carreras, N., Udelhoven, T., Krein, A., Gallart, F., Iffly, J.F., Ziebel, J., Hoffmann, L., Pfister, L., Walling, D.E., 2010c. The use of sediment colour measured by diffuse reflectance spectrometry to determine sediment sources: Application to the Attert River catchment (Luxembourg). J Hydrol (Amst) 382, 49–63. https://doi.org/10.1016/j.jhydrol.2009.12.017
Modernel, P., Rossing, W.A.H., Corbeels, M., Dogliotti, S., Picasso, V., Tittonell, P., 2016. Land use change and ecosystem service provision in Pampas and Campos grasslands of southern South America. Environmental Research Letters 11, 113002. https://doi.org/10.1088/1748-9326/11/11/113002
Oliveira, T.E. de, Freitas, D.S. de, Gianezini, M., Ruviaro, C.F., Zago, D., Mércio, T.Z., Dias, E.A., Lampert, V. do N., Barcellos, J.O.J., 2017. Agricultural land use change in the Brazilian Pampa Biome: The reduction of natural grasslands. Land use policy 63, 394–400. https://doi.org/10.1016/j.landusepol.2017.02.010
Overbeck, G.E., Muller, S., Fidelis, A., Pfadenhauer, J., Pillar, V.D., Blanco, C., Boldrini, I.I., Both, R., Forneck, E.D., 2007. Brazil's neglected biome: The South Brazilian Campos. Perspect Plant Ecol Evol Syst 9, 101–116. https://doi.org/10.1016/j.ppees.2007.07.005
Phillips, J.M., Russell, M.A., Walling, D.E., 2000. Time-integrated sampling of fluvial suspended sediment: A simple methodology for small catchments. Hydrol Process 14, 2589–2602. https://doi.org/10.1002/1099-1085(20001015)14:14<2589::AID-HYP94>3.0.CO;2-D
Pillar, V., Tornquist, C., Bayer, C., 2012. The southern Brazilian grassland biome: soil carbon stocks, fluxes of greenhouse gases and some options for mitigation. Brazilian Journal of Biology 72, 673–681. https://doi.org/10.1590/S1519-69842012000400006
Pulley, S., Collins, A.L., 2021. The potential for colour to provide a robust alternative to high-cost sediment source fingerprinting: Assessment using eight catchments in England. Science of The Total Environment 792, 148416. https://doi.org/10.1016/J.SCITOTENV.2021.148416
Pulley, S., Collins, A.L., Laceby, J.P., 2020. The representation of sediment source group tracer distributions in Monte Carlo uncertainty routines for fingerprinting: an analysis of accuracy and precision using data for four contrasting catchments. Hydrol Process 1–20. https://doi.org/10.1002/hyp.13736
Pulley, S., Van der Waal, B., Rowntree, K., Collins, A.L., 2018. Colour as reliable tracer to identify the sources of historically deposited flood bench sediment in the Transkei, South Africa: A comparison with mineral magnetic tracers before and after hydrogen peroxide pre-treatment. Catena (Amst) 160, 242–251. https://doi.org/10.1016/j.catena.2017.09.018
R Development Core Team, 2017. R: a language and environment for statistical computing.
Ramon, R., Evrard, O., Laceby, J.P., Caner, L., Inda, A. V., Barros, C.A.P. de, Minella, J.P.G., Tiecher, T., 2020. Combining spectroscopy and magnetism with geochemical tracers to improve the discrimination of sediment sources in a homogeneous subtropical catchment. Catena (Amst) 195, 104800. https://doi.org/10.1016/j.catena.2020.104800
Riddle, B., Fox, J., Mahoney, D.T., Ford, W., Wang, Y.T., Pollock, E., Backus, J., 2022. Considerations on the use of carbon and nitrogen isotopic ratios for sediment fingerprinting. Science of The Total Environment 817, 152640. https://doi.org/10.1016/J.SCITOTENV.2021.152640
Rodrigues, M.F., Reichert, J.M., Burrow, R.A., Flores, E.M.M., Minella, J.P.G., Rodrigues, L.A., Oliveira, J.S.S., Cavalcante, R.B.L., 2018. Coarse and fine sediment sources in nested

watersheds with eucalyptus forest. Land Degrad Dev 29, 2237–2253. https://doi.org/10.1002/ldr.2977
Roesch, L.F., Vieira, F., Pereira, V., Schünemann, A.L., Teixeira, I., Senna, A.J., Stefenon, V.M., 2009. The Brazilian Pampa: A Fragile Biome. Diversity (Basel) 1, 182–198. https://doi.org/10.3390/d1020182
Sánchez-Marañón, M., 2011. Color Indices, Relationship with Soil Characteristics, in: Gliński, J., Horabik, J., Lipiec, J. (Eds.), Encyclopedia of Agrophysics. Springer Netherlands, Dordrecht, pp. 141–145. https://doi.org/10.1007/978-90-481-3585-1_237
Sellier, V., Navratil, O., Laceby, J.P., Legout, C., Allenbach, M., Lefèvre, I., Evrard, O., 2020. Combining colour parameters and geochemical tracers to improve sediment source discrimination in a mining catchment (New Caledonia, South Pacific Islands). SOIL Discussions in review. https://doi.org/https://doi.org/10.5194/soil-2020-48
Smith, H.G., Blake, W.H., 2014. Sediment fingerprinting in agricultural catchments: A critical re-examination of source discrimination and data corrections. Geomorphology 204, 177–191. https://doi.org/10.1016/j.geomorph.2013.08.003
Stevenson, B.A., Kelly, E.F., McDonald, E. V., Busacca, A.J., 2005. The stable carbon isotope composition of soil organic carbon and pedogenic carbonates along a bioclimatic gradient in the Palouse region, Washington State, USA. Geoderma 124, 37–47. https://doi.org/10.1016/j.geoderma.2004.03.006
Tiecher, T., Minella, J.P.G., Caner, L., Evrard, O., Zafar, M., Capoane, V., Le Gall, M., Santos, D.R. dos, 2017. Quantifying land use contributions to suspended sediment in a large cultivated catchment of Southern Brazil (Guaporé River, Rio Grande do Sul). Agric Ecosyst Environ 237, 95–108. https://doi.org/10.1016/j.agee.2016.12.004
Tiecher, T., Minella, J.P.G., Evrard, O., Caner, L., Merten, G.H., Capoane, V., Didoné, E.J., dos Santos, D.R., 2018. Fingerprinting sediment sources in a large agricultural catchment under no-tillage in Southern Brazil (Conceição River). Land Degrad Dev 29, 939–951. https://doi.org/10.1002/ldr.2917
Uber, M., Legout, C., Nord, G., Crouzet, C., Demory, F., Poulenard, J., 2019. Comparing alternative tracing measurements and mixing models to fingerprint suspended sediment sources in a mesoscale Mediterranean catchment. J Soils Sediments 19, 3255–3273. https://doi.org/10.1007/s11368-019-02270-1
Valente, M.L., Reichert, J.M., Legout, C., Tiecher, T., Cavalcante, R.B.L., Evrard, O., 2020. Quantification of sediment source contributions in two paired catchments of the Brazilian Pampa using conventional and alternative fingerprinting approaches. Hydrol Process 34, 2965–2986. https://doi.org/10.1002/hyp.13768
Viglizzo, E.F., Ricard, M.F., Taboada, M.A., Vázquez-Amábile, G., 2019. Reassessing the role of grazing lands in carbon-balance estimations: Meta-analysis and review. Science of the Total Environment 661, 531–542. https://doi.org/10.1016/j.scitotenv.2019.01.130
Viscarra Rossel, R.A., Minasny, B., Roudier, P., McBratney, A.B., 2006. Colour space models for soil science. Geoderma 133, 320–337. https://doi.org/10.1016/j.geoderma.2005.07.017
Walling, D.E., 2013. The evolution of sediment source fingerprinting investigations in fluvial systems. J Soils Sediments 13, 1658–1675. https://doi.org/10.1007/s11368-013-0767-2
Wills, S.A., Burras, C.L., Sandor, J.A., 2007. Prediction of Soil Organic Carbon Content Using Field and Laboratory Measurements of Soil Color. Soil Science Society of America Journal 71, 380–388. https://doi.org/10.2136/sssaj2005.0384

Xu, Y., He, J., Cheng, W., Xing, X., Li, L., 2010. Natural 15N abundance in soils and plants in relation to N cycling in a rangeland in Inner Mongolia. Journal of Plant Ecology 3, 201–207. https://doi.org/10.1093/jpe/rtq023
Zaimes, G.N., Tufekcioglu, M., Schultz, R.C., 2019. Riparian land-use impacts on stream bank and gully erosion in agricultural watersheds: What we have learned. Water (Switzerland) 11. https://doi.org/10.3390/w11071343

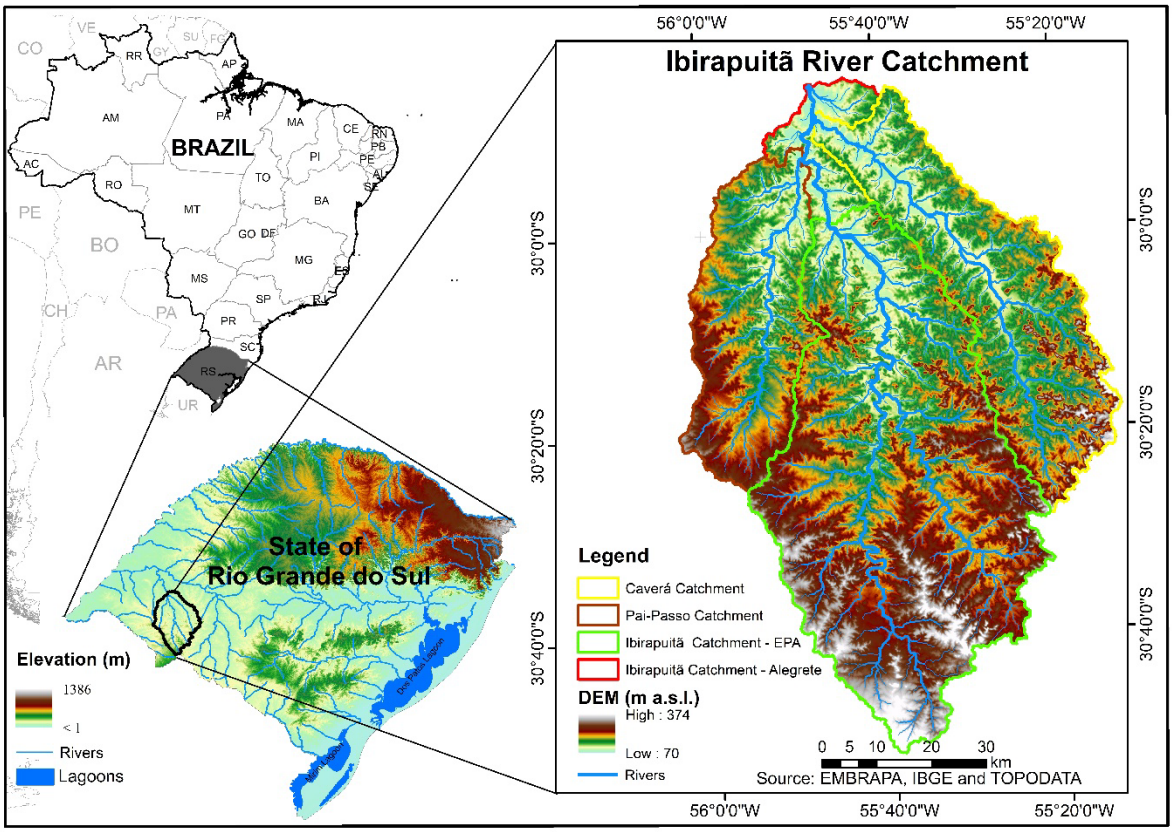

Figure 1.
Location of the Ibirapuitã River catchment in South Brazil highlighting the digital elevation model (DEM), the river drainage network, and the limits of the three main sub-basins monitored (Caverá, Pai-Passo, and environmental protection area (EPA) sub-catchemnts).

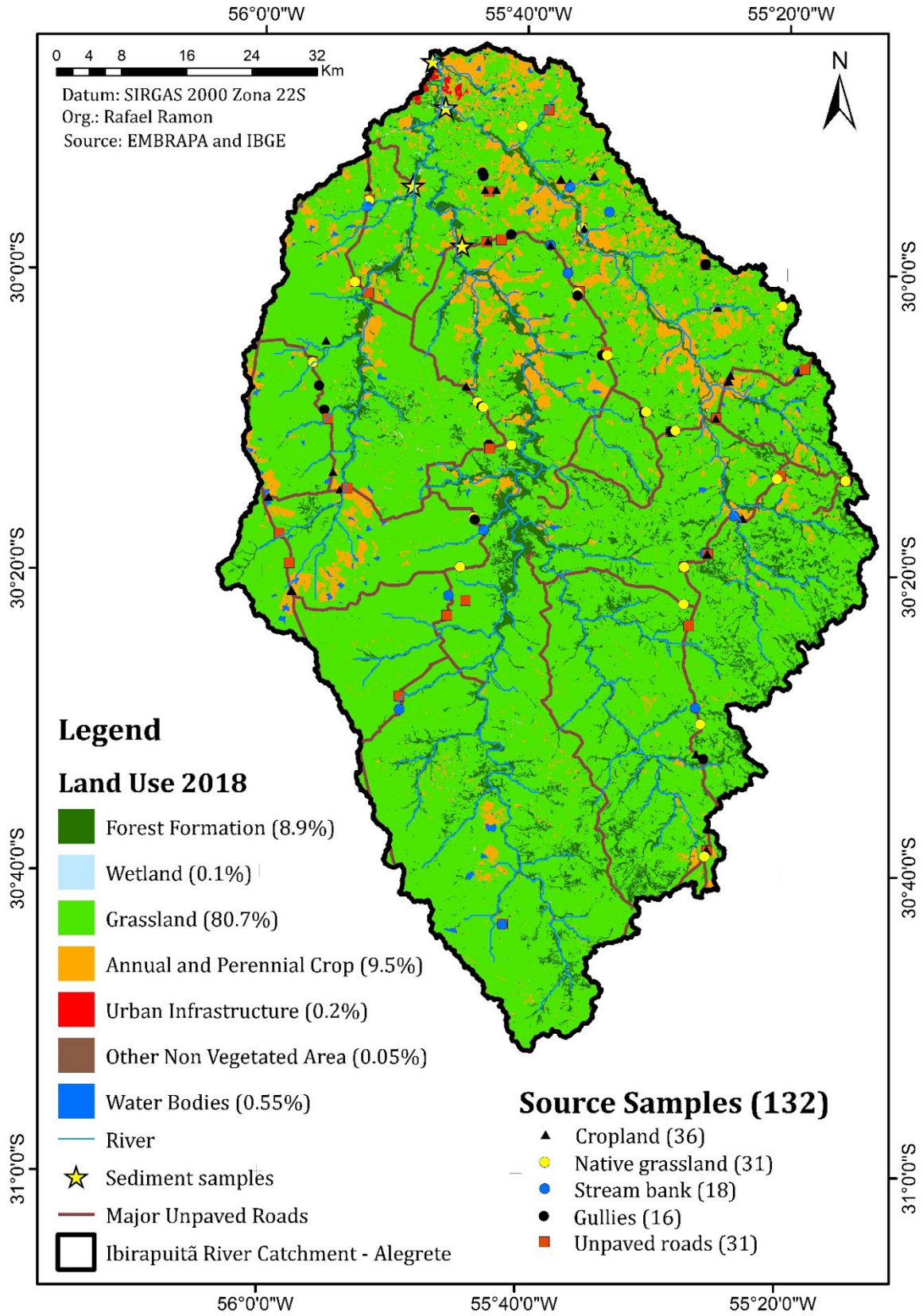

Figure 2.
Distribution of land use and sampling sites for suspended sediments and sediment sources characterization in the Ibirapuitã River catchment.

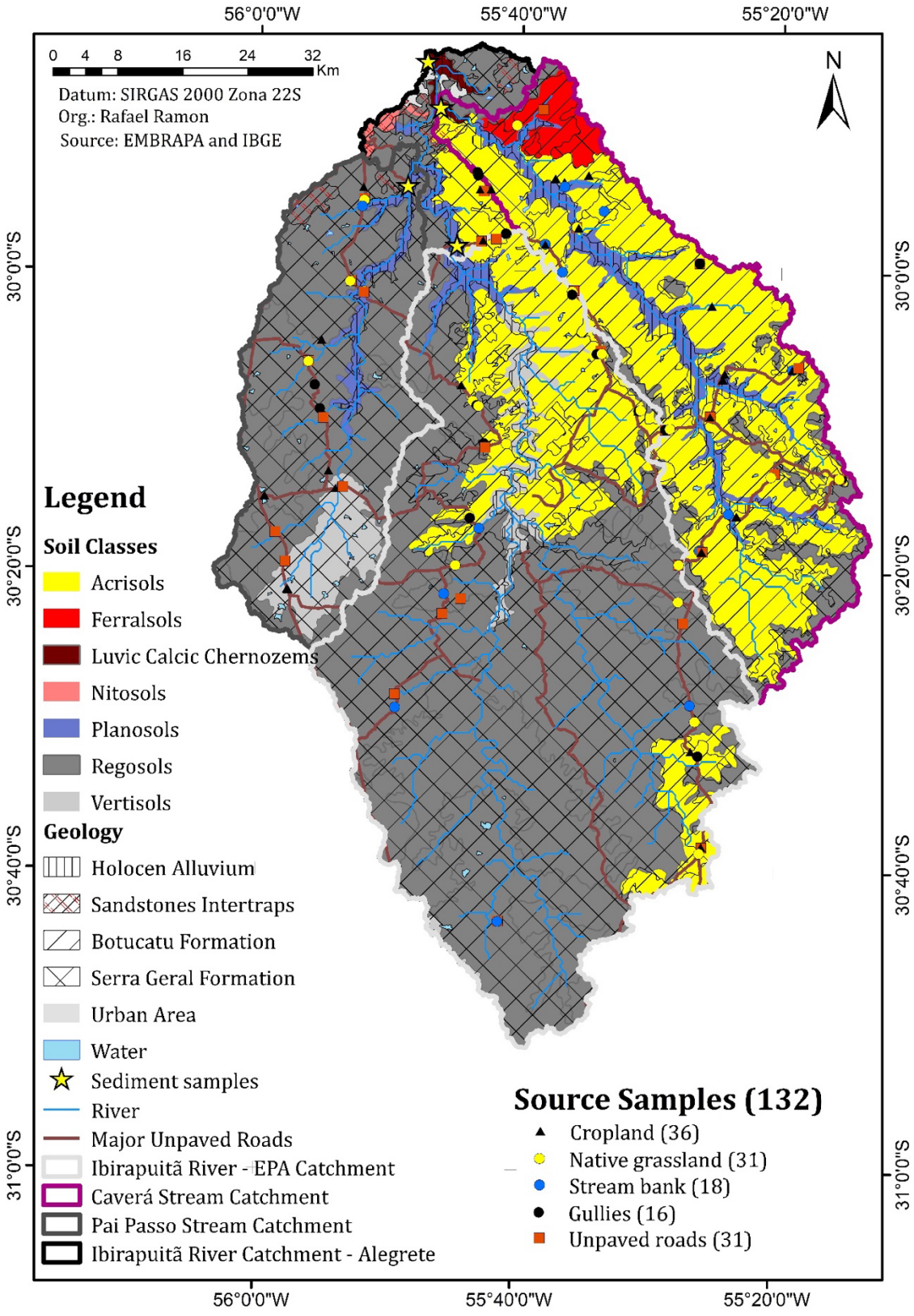

Figure 3.
Soil types, geology, and sampling sites in the Ibirapuitã River catchment.

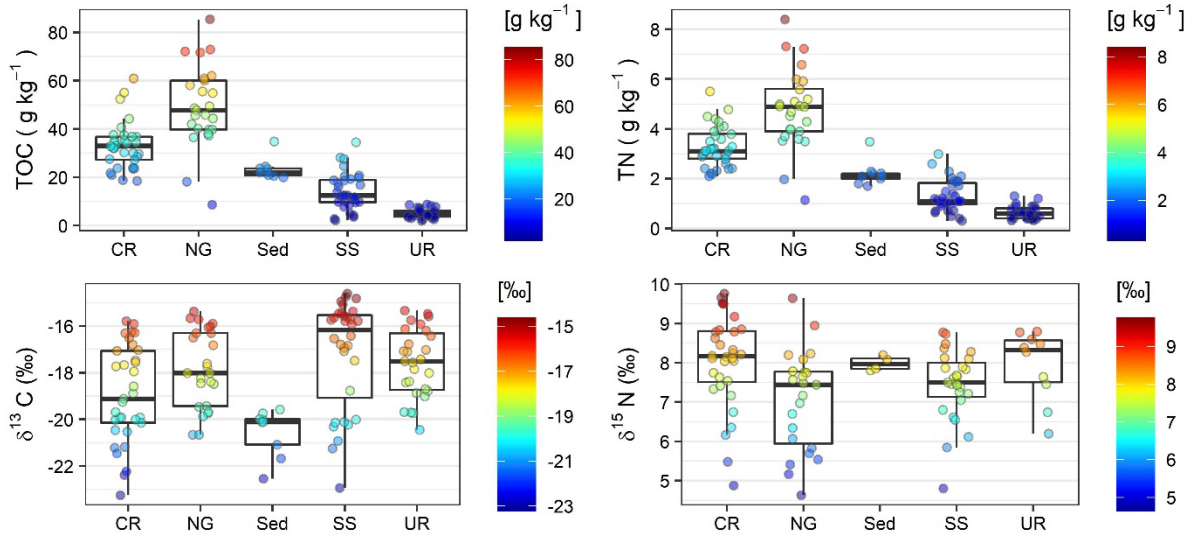

Figure 4.

Boxplots of total organic carbon (TOC), total nitrogen (TN), and $\delta^{13}C$ and $\delta^{15}N$ isotope ratio in the potential sources and sediment samples. CR, croplands; NG, native grasslands; Sed, sediment samples; SS, subsurface sources; UR, unpaved roads.

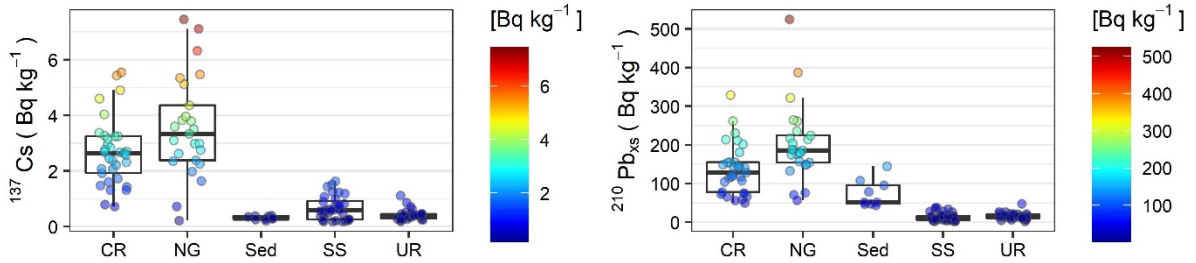

Figure 5.

Boxplots of fallout radionuclide activities (^{137}Cs and $^{210}Pb_{xs}$) for potential sources and sediment samples. CR, croplands; NG, native grasslands; Sed, sediment samples; SS, subsurface sources; UR, unpaved roads.

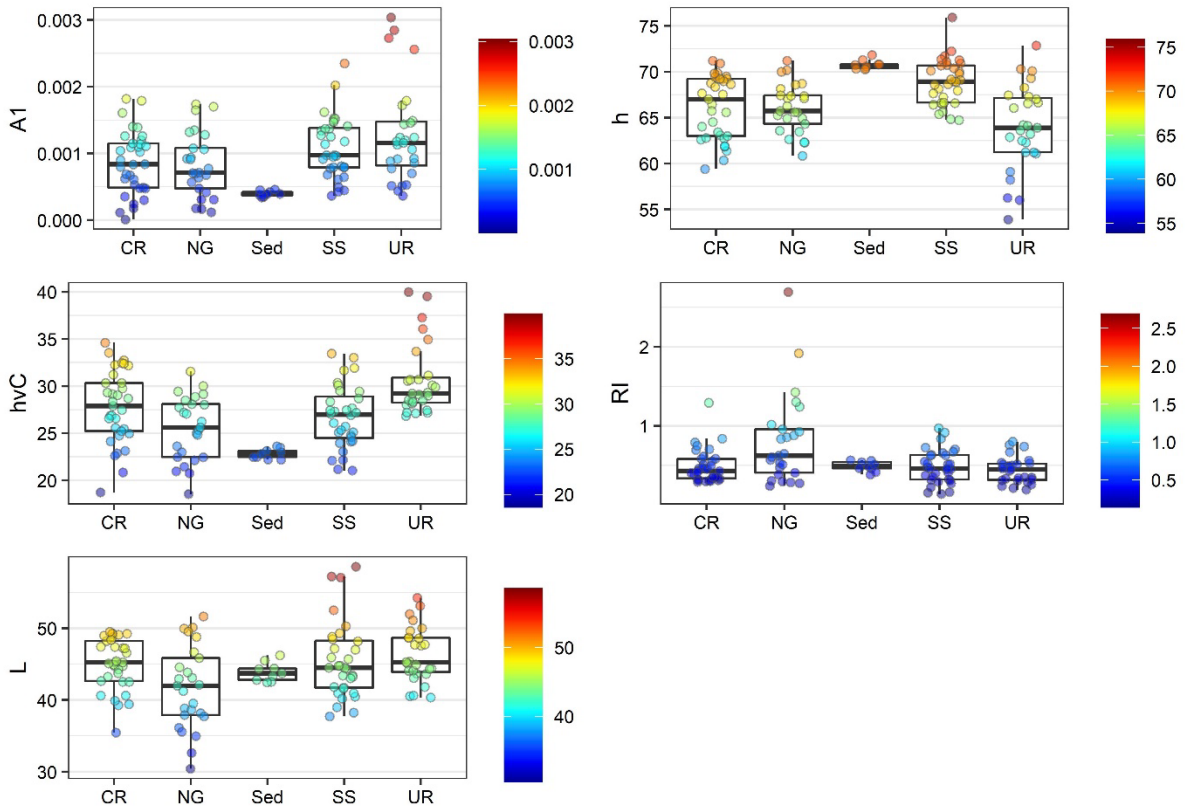

Figure 6.
Boxplots of UV derived parameters in potential sources and sediment samples. CR, croplands; NG, native grasslands; Sed, sediment samples; SS, subsurface sources; UR, unpaved roads. This figure only contains five UV derived parameters selected by the LDA from a total of 30 parameters measured.

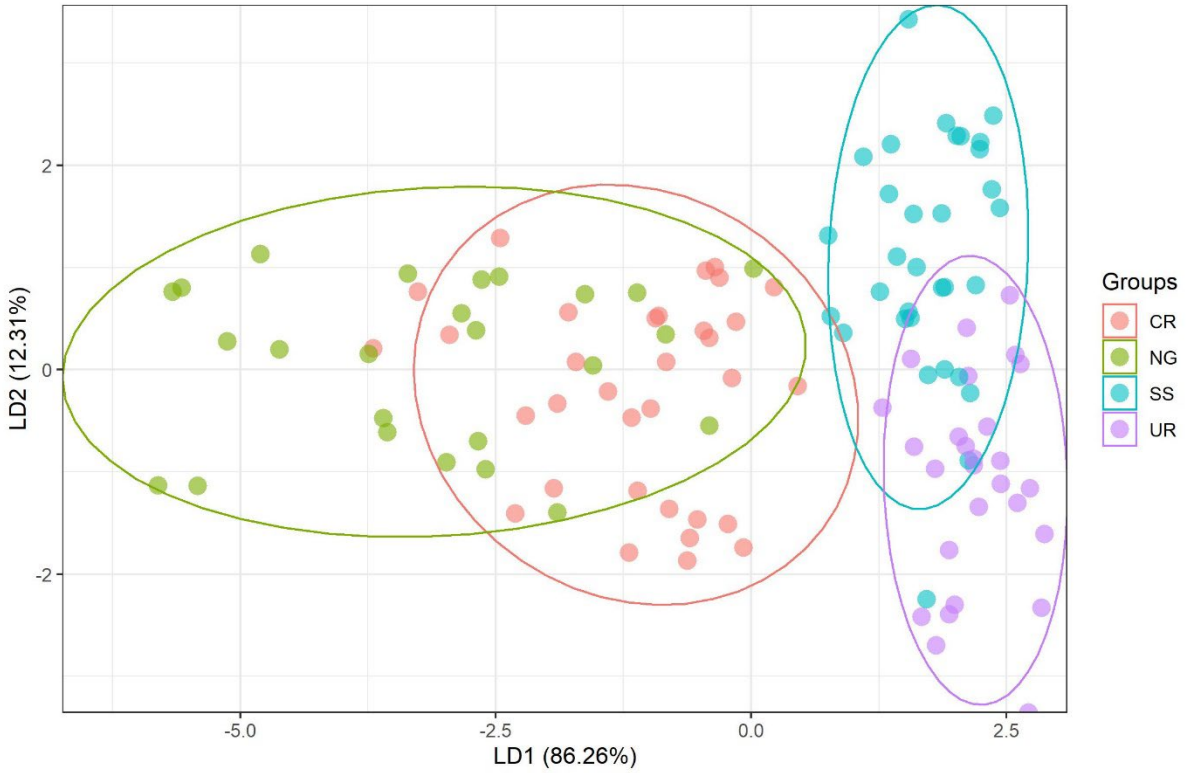

Figure 7.
Source sample reclassification by the linear discriminant analysis using the selected set of tracers (TN, h, $^{210}Pb_{xs}$, A1, hvC, RI, and L). CR, croplands; NG, native grasslands; SS, subsurface sources; UR, unpaved roads; LD1, first linear discrimination function; LD2, second linear discrimination function.

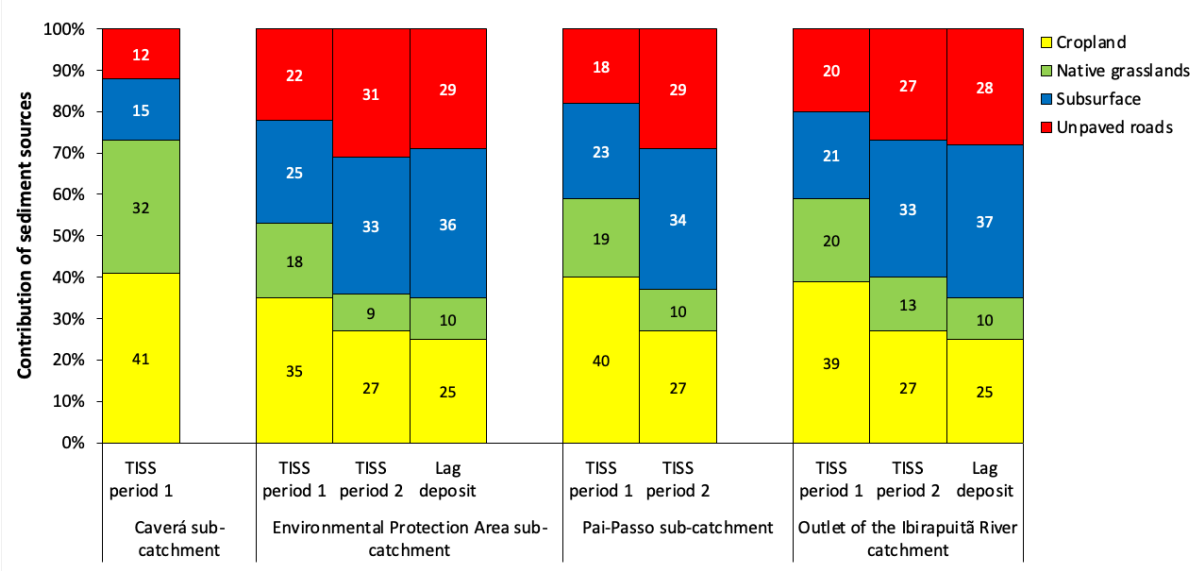

Figure 8.
Mean sediment source contribution for the individual sediment samples collected in the Ibirapuitã River catchment. TISS, time integrated suspended sediment sample; Lag, Lag deposit sample.

Table 1. Mean values, standard deviation, and non-parametric comparison of potential tracers evaluated in four main sources of sediments (cropland, native grasslands, subsurface, and unpaved roads), maximum and minimum values in the sediment sources, and mean value and standard deviation of potential tracers in the sediments sampled in the Ibirapuitã River catchment, South Brazil.

Fingerprint property	Croplands	Native grasslands	Subsurface	Unpaved road	Sources	
	Mean	Mean	Mean	Mean	Max	Min
	n = 33	n = 26	n = 31	n = 27	n = 117	
^{137}Cs (Bq kg^{-1})	2.66 ± 1.23	3.35 ± 1.65	0.67 ± 0.44	0.43 ± 0.2	7.45	0.18
$^{210}Pb_{xs}$ (Bq kg^{-1})	136.73 ± 63.46	197.67 ± 101.26	14.99 ± 10.58	16.17 ± 9.04	524.56	1.77
TN (g kg^{-1})	3.3 ± 0.85	4.47 ± 1.52	1.35 ± 0.63	0.63 ± 0.27	0.73	0.03
TOC (g kg^{-1})	32.75 ± 9.12	46.24 ± 16.12	14.52 ± 7.63	5.07 ± 1.95	7.29	0.19
CN Ratio	9.89 ± 0.8	10.28 ± 1.08	10.47 ± 2.36	8.15 ± 1.3	16.80	5.30
$\delta^{13}C$ (‰)	-19 ± 2.01	-17.79 ± 1.62	-17.2 ± 2.34	-17.59 ± 1.47	-14.61	-23.25
$\delta^{15}N$ (‰)	8.11 ± 1.05 (n=27)	7.07 ± 1.3 (n=25)	7.44 ± 0.9 (n=28)	7.94 ± 0.9 (n=14)	9.76	4.63
A1	0.00086 ± 0.00049	0.00087 ± 0.00045	0.00109 ± 0.00047	0.00129 ± 0.00075	0.00304	0.00001
A2	0.00024 ± 0.00011	0.00029 ± 0.00012	0.00034 ± 0.00019	0.00031 ± 0.00008	0.00077	0.00007
A3	0.00031 ± 0.00024	0.00026 ± 0.00016	0.00022 ± 0.00006	0.00048 ± 0.00042	0.00169	0.00005
Hr	0.29 ± 0.15	0.24 ± 0.07	0.18 ± 0.04	0.25 ± 0.07	0.83	0.11
L*	52.35 ± 3.2	48.62 ± 5.85	52.08 ± 4.81	53.38 ± 3.81	63.95	36.48
a*	9.32 ± 3.17	8.21 ± 2.12	7.68 ± 1.83	11.8 ± 4.32	21.91	4.76
b*	20.55 ± 4.2	18.43 ± 3.48	19.57 ± 3.91	23.39 ± 3.93	32.79	11.69
C*	22.6 ± 5.08	20.2 ± 3.95	21.04 ± 4.23	26.29 ± 5.39	39.44	12.82
h	66.17 ± 3.43	66.18 ± 2.72	68.64 ± 2.16	63.91 ± 4.66	72.86	53.90
x	0.39 ± 0.02	0.39 ± 0.01	0.39 ± 0.01	0.41 ± 0.02	0.46	0.36
y	0.38 ± 0.01	0.38 ± 0.01	0.38 ± 0.01	0.38 ± 0	0.39	0.36
z	0.23 ± 0.02	0.24 ± 0.02	0.24 ± 0.02	0.21 ± 0.03	0.27	0.16
L	45.27 ± 3.16	41.7 ± 5.64	45.04 ± 4.83	46.3 ± 3.82	57.22	30.43
a	7.66 ± 2.72	6.54 ± 1.8	6.26 ± 1.63	9.81 ± 3.67	18.68	3.67
b	13.14 ± 2.44	11.62 ± 2.29	12.64 ± 2.56	14.7 ± 1.89	18.81	6.89
u*	24.12 ± 6.79	21.01 ± 4.85	21.17 ± 4.72	29.32 ± 8.21	49.41	12.40
v*	23.42 ± 4.22	20.86 ± 3.97	22.7 ± 4.48	26.01 ± 3.18	32.84	12.58
u’	0.23 ± 0.01	0.23 ± 0.01	0.23 ± 0.01	0.24 ± 0.01	0.27	0.22
v’	0.5 ± 0.01	0.5 ± 0	0.5 ± 0	0.51 ± 0	0.52	0.49
RI	0.47 ± 0.16	0.8 ± 0.56	0.5 ± 0.21	0.44 ± 0.17	2.69	0.16
Hvc	198.64 ± 11.24	200.32 ± 8.31	205 ± 6.36	190.56 ± 14.15	215.82	158.24
hVc	29.56 ± 1.46	27.86 ± 2.67	29.43 ± 2.19	30.03 ± 1.74	34.85	22.32
hvC	27.88 ± 3.66	25.58 ± 3.26	26.64 ± 3.32	30.63 ± 3.78	39.99	18.54
R	147.86 ± 15.41	144.26 ± 11.46	141.77 ± 9.95	159.41 ± 20.22	205.34	123.20
G	85.87 ± 2.26	86.14 ± 1.6	87.51 ± 1.18	83.95 ± 4.42	90.14	72.54

B	47.69 ± 6.4	49.35 ± 5.04	49.32 ± 5.08	43.4 ± 6.72	59.94	28.38
HRGB	5.95 ± 3.36	5.33 ± 2.37	4.02 ± 1.66	8.73 ± 5.6	22.59	1.50
IRGB	93.81 ± 2.38	93.25 ± 1.77	92.87 ± 1.54	95.59 ± 3.12	102.66	89.99
SRGB	50.08 ± 10.88	47.46 ± 8.22	46.23 ± 7.47	58 ± 13.43	88.33	31.63
CI	0.26 ± 0.06	0.25 ± 0.04	0.24 ± 0.04	0.31 ± 0.07	0.48	0.17
SI	0.51 ± 0.09	0.49 ± 0.07	0.48 ± 0.07	0.57 ± 0.09	0.76	0.35

Table 2. Summary of linear discriminant analysis (LDA) outputs.

Selected tracers	TN, h, $^{210}Pb_{xs}$, A1, hvC3, RI, L
Wilk's Lambda	0.09
Variance explained by the variables (%)	91.1
Squared Mahalanobis distances	
Croplands × Native grasslands	4.5
Croplands × Subsurface	11.6
Croplands × Unpaved road	12.5
Native grasslands × Subsurface	25.5
Native grasslands × Unpaved road	29.7
Subsurface × Unpaved road	5.3
Average	14.8
p-levels	
Croplands × Native grasslands	<0.001
Croplands × Subsurface	<0.001
Croplands × Unpaved road	<0.001
Native grasslands × Subsurface	<0.001
Native grasslands × Unpaved road	<0.001
Subsurface × Unpaved road	<0.001
Source samples correctly classified (%)	
Croplands	84.8
Native grasslands	76.0
Subsurface	84.4
Unpaved road	85.2
Average	82.9
Uncertainty associated with the discrimination of the source (%)	
Croplands	24.6
Native grasslands	28.4
Subsurface	20.2
Unpaved road	18.9
Average	23.0